Anomalous phenomenon of a focused evanescent Laguerre-Gaussian beam

Baohua Jia, Xiaosong Gan, and Min Gu

Centre for Micro-Photonics, Faculty of Engineering and Industrial Sciences, Swinburne University of Technology, P.O. Box 218 Hawthorn, 3122 Australia
xgan@swin.edu.au

Abstract: We demonstrate theoretically and experimentally an anomaly in the intensity distribution at the focal region of a Laguerre-Gaussian beam, when such a beam is focused by a high numerical aperture objective lens through an index-mismatched interface satisfying the total internal reflection condition. An asymmetric rotation of the focal field arising from the interplay of the phase shift induced by the total internal reflection and the helical phase of the Laguerre-Gaussian beam has been experimentally observed by a scanning near-field optical microscope. A cross-section analysis shows that the experimental results match well with the theoretical predictions.

© 2005 Optical Society of America

OCIS codes: (260.1960) Diffraction theory; (110.0180) Microscopy, (140.7010) Trapping; (230.3720) Liquid-crystal devices

References and links

1. M. Tokunaga, K. Kitamura, K. Saito, A. H. Iwane and T. Yanagida, Biochem. "Single molecule imaging of fluorophores and enzymatic reactions achieved by objective-type total internal reflection fluorescence microscopy," Biophys. Res. Commun. **235**, 47-53 (1997).
2. J. W. M. Chon and M. Gu, "Scanning total internal reflection fluorescence microscopy under one-photon and two-photon excitation: image formation," Appl. Opt. **43**, 1063-1071 (2004).
3. N. Hayazawa, A. Tarun, Y. Inouye, and S. Kawata, "Near-field enhanced Raman spectroscopy using side illumination optics," J. Appl. Phys. **92**, 6983-6986 (2002).
4. B. Sick, B. Hecht, and L. Novotny, "Orientational imaging of single molecules by annular illumination, " Phys. Rev. Lett. **85**, 4482-4485 (2000).
5. M. Gu, J.-B. Haumonte, Y. M., J. W. M. Chon, and X. Gan, "Laser trapping and manipulation under focused evanescent wave illumination," Appl. Phys. Lett. **84**, 4236-4238 (2004).
6. D. Ganic, X. Gan, and Min Gu, "Trapping force and optical lifting under focused evanescent wave illumination," Opt. Express **12**, 5533-5538 (2004), http://www.opticsexpress.org/abstract.cfm?URI=OPEX-12-22-5533.
7. D. Ganic, X. Gan, and M. Gu, "Optical trapping force with annular and doughnut laser beams based on vectorial diffraction," Opt. Express **13,** 1260-1265 (2005), http://www.opticsexpress.org/abstract.cfm?URI=OPEX-13-4-1260.
8. K. Okamoto and S. Kawata, "Radiation force exerted on subwavelength particles near a nanoaperture," Phys. Rev. Lett. **83**, 4534-4537 (1999).
9. L. Novotny, R. X. Bian, and X. S. Xie, "Theory of nanometric optical tweezers," Phys. Rev. Lett. **79**, 645-648 (1997).
10. B. Jia, X. Gan, and M. Gu, "Direct measurement of a radially polarized focused evanescent field facilitated by a single LCD, " Opt. Express **13**, 6821-6827 (2005), http://www.opticsexpress.org/abstract.cfm?URI=OPEX-13-18-6821.
11. H. H. Hopkins, "The airy disc formula for systems of high relative aperture," Proc. Phys. Soc. **55,** 116-128 (1943).
12. B. Jia, X. Gan, and M. Gu, "Direct observation of a pure focused evanescent field of a high numerical aperture objective lens by scanning near-field optical microscopy," Appl. Phys. Lett. **86**, 131110, (2005).
13. S. K. Rhodes, K. A. Nugent, and A. Roberts, "Precision measurement of the electromagnetic fields in the focal region of a high-numerical-aperture lens using a tapered fiber probe," J. Opt. Soc. Am. A **19**, 1689-1693 (2002).
14. K. Bahlmann and S. W. Hell, "Electric field depolarization in high aperture focusing with emphasis on annular apertures," J. of Microsc. **200**, 59-67 (2000).

#8834 - $15.00 USD Received 20 September 2005; revised 4 December 2005; accepted 5 December 2005
(C) 2005 OSA

15. K. S. Youngworth and T. G. Brown, "Focusing of high numerical aperture cylindrical-vector beams," Opt. Express **7**, 77-87 (2000), http://www.opticsexpress.org/abstract.cfm?URI=OPEX-7-2-77.
16. H. He, M. E. J. Friese, N. R. Heckenberg, and H. Rubinsztein-Dunlop, "Direct observation of transfer of angular momentum to absorptive particles from a Laser beam with a phase singularity," Phys. Rev. Lett. **75**, 826-829 (1995).
17. M. P. MacDonald, L. Paterson, K. Volke-Sepulveda, J. Arlt, W. Sibbett, and K. Dholakia, "Creation and manipulation of three-dimensional optically trapped structures," Science **296**, 1101-1103 (2002).
18. L. Paterson, M. P. MacDonald, J. Arlt, W. Sibbett, P. E. Bryant, and K. Dholakia, "Controlled rotation of optically trapped microscopic particles," Science **292**, 912-914 (2001).
19. D. G. Grier, "A revolution in optical manipulation," Nature **424**, 810-816 (2003).
20. D. W. Zhang and X.-C. Yuan, "Optical doughnut for optical tweezers**,"** Opt. Lett. **28**, 740-742 (2003).
21. D. Ganic, X. Gan, and M. Gu, "Focusing of doughnut laser beams by a high numerical-aperture objective in free space," Opt. Express **11**, 2747-2752 (2003), http://www.opticsexpress.org/abstract.cfm?URI=OPEX-11-21-2747.
22. E. Hecht and A. Zajac, *Optics* (Addison-Wesley Publishing Company, U. S. A, 2002)
23. M. Gu, *Advanced Optical Imaging Theory* (Springer, Heidelberg, 2000).
24. P. Torok, P. Varga, Z. Laczik, and G. R. Booker, "Electromagnetic diffraction of light focused through a planar interface between materials of mismatched refractive indices: an integral representation," J. Opt. Soc. Am. A, **12,** 325-332 (1995).
25. C. A. Alonzo, P. J. Rodrigo, and J. Glückstad, "Helico-conical optical beams: a product of helical and conical phase fronts," Opt. Express **13,** 1749-1760 (2005), http://www.opticsexpress.org/abstract.cfm?URI=OPEX-13-5-1749.

1. Introduction

Generation of a focused evanescent field using a high numerical aperture (NA) total internal reflection (TIR) objective lens has been proposed and demonstrated extensively recently because of its enormous applications in the fields of near-field microscopy, spectroscopy and near-field optical trapping [1-7]. Compared with other methods, such as utilizing nano-apertures [8] or surface plasmon enhanced metal tips [9], using a high NA objective lens to generate a strongly localized evanescent field has some unique advantages. For example, it can not only eliminate the difficulties associated with the sample-probe distance control, but also reduce the heating effect, which is crucial especially in the field of optical trapping. Most important of all, it allows the dynamic modulation of the focal distribution by controlling the wavefront entering the objective lens [10]. It is well known that when a plane wave is focused by a low NA objective, a circularly symmetric Airy-spot-like focal spot always presents in the focal region of the objective [11]. However, with increasing the NA of the objective lenses, such a focal pattern disappears due to the breakdown of the paraxial condition. As a result, a focus elongation or splitting is expected in the focal region of a high NA objective, especially when the illuminating beam satisfies the TIR condition [2,5,12]. The phenomenon is so called focus depolarization due to the fact that a longitudinal polarization component arises in the focal region of the objective [13-15].

Because of carrying orbital angular momentum, Laguerre-Gaussian (LG) beams, also known as the doughnut beams due to their characteristic intensity distributions of a dark spot on the optical axis surrounded by a bright ring, have been extensively employed in many novel optical trapping experiments [16-20]. The focusing properties of LG beams by a high NA objective have also attracted lots of research interests [21]. It has been revealed recently that when focused by a high NA objective lens in free space, the LG beams lose their central zero intensities for lower topological charge (n) cases due to the presence of the longitudinal polarization component in the focal region. Moreover, two distinctive intensity maxima appear in the direction perpendicular to the incident polarization direction resulting in the breakdown of the radial symmetry. It was pointed out that such an asymmetric phenomenon could cause significant influence on optical trapping and super-resolution optical microscopy. The intensity distribution deformation is expected to be more pronounced when an index-mismatched interface is presented.

#8834 - $15.00 USD Received 20 September 2005; revised 4 December 2005; accepted 5 December 2005
(C) 2005 OSA

In this paper, the intensity distributions in the focal region of LG beams focused by a high NA objective operating when the illuminating beam satisfies the TIR condition are calculated using the vectorial Debye theory and experimentally mapped with a scanning near-field optical microscope (SNOM). A new anomalous phenomenon, which shows a rotation of the focal field, is demonstrated. It has been revealed that such anomalous focal field distributions of the evanescent LG beams are intrinsic phenomena in all the objectives illuminated by LG beams undergo the TIR condition.

2. Theoretical results

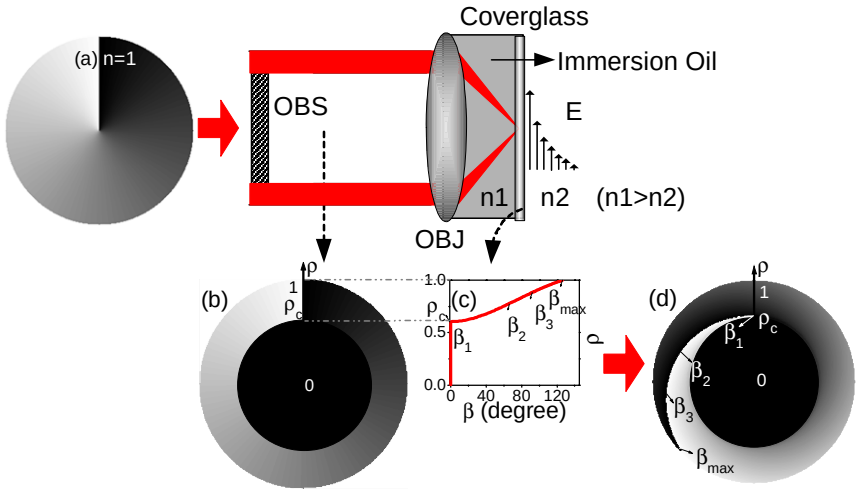

Fig. 1. Schematic for the phase shift generated by a high NA objective (NA=1.65, 100×) at the coverglass (n_1=1.78) and air (n_2=1) interface under the TIR condition and its interaction with the helical phase pattern of an LG beam (n=1). (a) Incident helical phase front of the LG beam, (b) obstructed by a circular opaque disk (OBS) to produce a focused evanescent field (ρ is the radius of the obstruction disk normalized by the size of the back aperture of the objective (OBJ). ρ_c is the critical radius, corresponding to the critical angle (θ_c in this case)), (c) phase shift β induced by TIR versus the normalized obstruction radius ρ. (d) Equivalent phase dislocation of the LG beam at the back aperture of the objective after adding up the phase shift β shown in (c).

The phase ramp for generating the LG beams can be expressed as $n\varphi$, where n is called the topological charge and φ is the polar coordinate in the plane perpendicular to the beam axis. An example of the phase pattern for n=1 is shown in Fig. 1(a). In order to produce a focused evanescent LG beam, a high NA TIR objective (NA=1.65) with a central obstruction disk is employed. The obstruction disk is inserted at the back aperture of the objective in such a way that only the illuminating beam with a convergence angle greater than the critical angle (θ_c=34.18° in our case) is allowed to enter the back aperture, as shown in Fig. 1(a). The obstructed helical phase pattern of the LG beam at the back aperture of the objective is shown in Fig. 1(b). When focused by the TIR objective, a phase shift β, as shown in Fig. 1(c), which can be determined by the Fresnel equation [22] under the TIR condition, is induced by the boundary effect and added on to the helical phase pattern. As a result, a phase dislocation φ_d, as shown in Fig. 1(d), is presented at the interface. Such a phase dislocation can be expressed, equivalently at the back aperture of the objective, as

$$\varphi_d = n\varphi + \beta(\rho) \qquad \rho_c < \rho < 1 \tag{1}$$

and it will definitely cause some variations to the focal field distributions.

#8834 - $15.00 USD Received 20 September 2005; revised 4 December 2005; accepted 5 December 2005
(C) 2005 OSA

The electric field distribution of a linearly polarized LG beam focused by a high NA objective through an index-mismatched interface has been calculated using the vectorial Debye theory [23,24]. Figs. 2(a-d) depict the normalized intensity distributions in the focal plane of the objective (NA=1.65) under the illumination of annular LG beams (n=0-3) at the coverglass (n_1=1.78) and air (n_2=1.0) interface. In this case, an obstruction disk with a size of $\rho = 0.803$, which is much larger than the critical radius $\rho_c = 0.6$, has been applied to match the experimental condition. It has been found in Fig. 2(a) that when the objective is illuminated by a Gaussian beam (n=0), the focal spot slightly splits along the incident polarization direction due to the presence of the longitudinal component in the focal region caused by the focusing of a high NA objective [13-15]. This result is consistent with the published results [2,5,12]. It should be pointed out that for the far-field focusing of a doughnut beam, although the radial symmetry is broken due to the depolarization effect, the symmetry with respect to the axis, which is perpendicular to the polarization direction of the illumination, still remains. However, when focused by a TIR objective, even such a symmetry cannot be sustained. It is interesting to note that when an LG beam of topological charge 1 is applied, an anomalous intensity distribution occurs in the focal region, as shown in Fig. 2(b). Two high intensity spots orients in the direction with a certain angle to the normal direction of the incident polarization are observed instead of a symmetric doughnut shaped bright ring [21]. Furthermore, when the beams of topological charges of n=2 and 3 are applied, spiral intensity patterns, which have the shapes similar to the optical spanner [19], are observed in the focal region of the objective. Apart from the asymmetry of the intensity distributions, the central zero intensities have disappeared for LG beams of n=1 and 2 (Figs. 2(b) and (c)) because of the contribution from the longitudinal polarization component in the focal region. However it reappears when n=3 (Fig. 2(d)), which is consistent with the focal field distribution of LG beams obtained in the far field high NA cases [21].

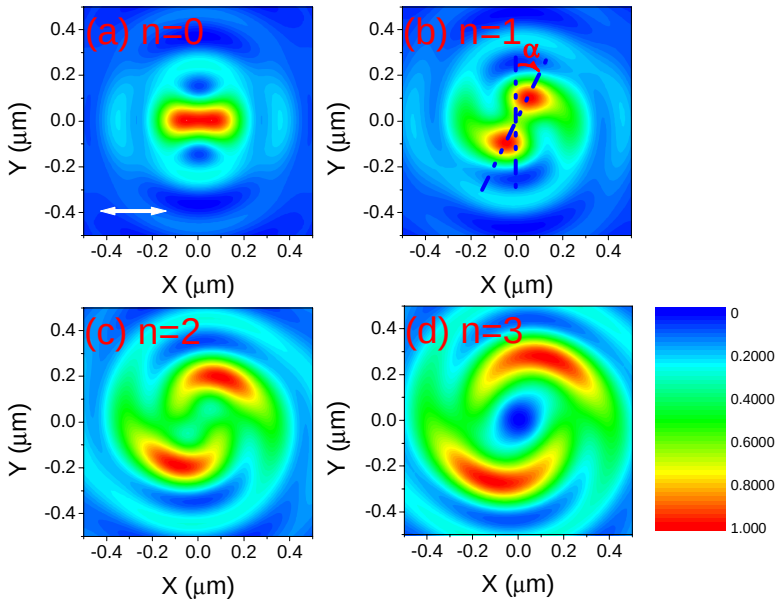

Fig. 2. Intensity distributions in the focal region of the objective (NA=1.65) at the coverglass (n_1=1.78) and air (n_2=1) interface under the illumination of LG beams with topological charges (a) n=0, (b) n=1, (c) n=2, (d) n=3. Each Fig. has been normalized to its maximum intensity. The arrow indicates the incident polarization direction.

#8834 - $15.00 USD Received 20 September 2005; revised 4 December 2005; accepted 5 December 2005
(C) 2005 OSA

3. Experimental results

To verify the theoretical findings, a SNOM (NT-MDT, Solver), which has the advantage of high spatial resolution and the ability to capture the near-field signals, is employed to map the focused evanescent field under the illumination of LG beams. The experimental setup (Fig. 3 (a)) for the characterization of focused evanescent LG beams is similar to that used for the characterization of a focused evanescent wave under the plane wave illumination [12] with the addition of a computer controlled spatial light modulator (SLM) (Hamamatsu PPM X8267 Series), which is used to generate the required helical phase pattern (Fig. 3(b)) for the LG beams. The SLM is capable of generating a phase-ramp with 256 gray levels, which is sufficient to produce LG beams with high quality. A high NA TIR objective (Olympus, NA=1.65, 100×) is used to focus the LG beams to a coverglass (n_1=1.78) and air (n_2=1) interface. An obstruction disk with a size of $\rho = 0.803$ was used to ensure the pure evanescent field in the focal region. In the detection arm, a confocal pinhole, located in front of a photo-multiplier tube (PMT), provides optical sectioning properties and is utilized to ensure the center of the focal spot is placed at the coverglass-air interface. The tightly focused evanescent field is directly mapped by a tiny aperture (30-100 nm in diameter) located at the top of an aluminum coated fiber tip of the SNOM. The distance between the fiber tip and the coverglass surface is controlled by the shear force mechanism. A charge-coupled device (CCD) is utilized to visualize the accurate position of the fiber probe in the close vicinity of the highly localized focal spot of the objective.

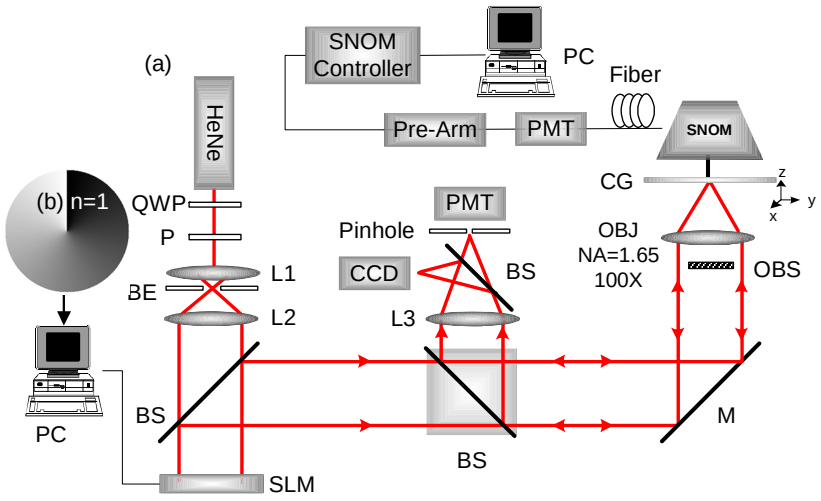

Fig. 3. (a) The experimental setup for the characterization of focused evanescent LG beams with a SNOM probe. QWP: quarter wave plate, P: polarizer, BE: beam expansion system, SLM: special light modulator, BS: beam splitter, M: mirror, L1, L2, L3: lenses, OBS: obstruction (ε=0.803), OBJ: objective, NA=1.65, 100×, CG: special coverglass (n=1.78) mounted on top of a three-dimensional scanning stage, Pre-Arm: pre-amplifier, CCD: charge-coupled device. (b) Phase pattern loaded on the SLM to generate a doughnut beam with topological charge 1.

Figsures 4(a) – 4(d) present a quantitative comparison between the experimental results and the theoretical simulations. The measured intensity distributions in the focal plane of the objective at the coverglass-air interface illuminated by LG beams with topological charges from 0 to 3 are shown in Fig. 4 insets on the left column. In comparison, the theoretical plots are shown on the right side of each figure. The measured intensity patterns for all the topological charges are in good match with the theoretical results. For example, the central singularity has also been vanished for the intensity distributions of focused LG beams for

#8834 - $15.00 USD Received 20 September 2005; revised 4 December 2005; accepted 5 December 2005
(C) 2005 OSA

n=1, 2; and it reappears for n=3. In addition, the experimental results confirm that the two peak intensity lobes rotate by a certain angle from their original direction, which is normal to the incident polarization direction. If a rotation angle α is defined as illustrated in Fig. 2(b), it can be found that the theoretical rotation angle, 26.5 degrees for n=2, is comparable to the experimental result, approximately 23 degrees.

A cross-section is drawn along the line that joins the two maximum intensity points. It has been found that the measured full width at the half maximum (FWHM) of the intensity distribution for n=0 is approximately 410 nm, which matches well with the theoretical predicted value (360 nm) after considering that the measured intensity distribution is approximately equal to the convolution of the finite probe size (approximately 60 nm) and the actual intensity distribution [12]. In addition, a good agreement on the separation of the two intensity peaks has also been found between the measurements and the theoretical predictions. For example, the separation of the two intensity peaks is 650 nm in experimental measurements for the case of n=3, which matches well with the calculated values 610 nm. However, some deviations can be observed in Figs. 4(a) and (b) in the middle dip ratio, which is defined as the ratio between the minimum value of the dip to its peak intensity. For instance, the measured middle dip ratio is 0.8 for n=1, while the theoretical value is 0.63. This small deviation between the experiment and theory can be attributed to the dominant longitudinal component in the total field and its higher coupling efficiency to the aluminum coated fiber probe, which makes it easier to be detected by the SNOM [12].

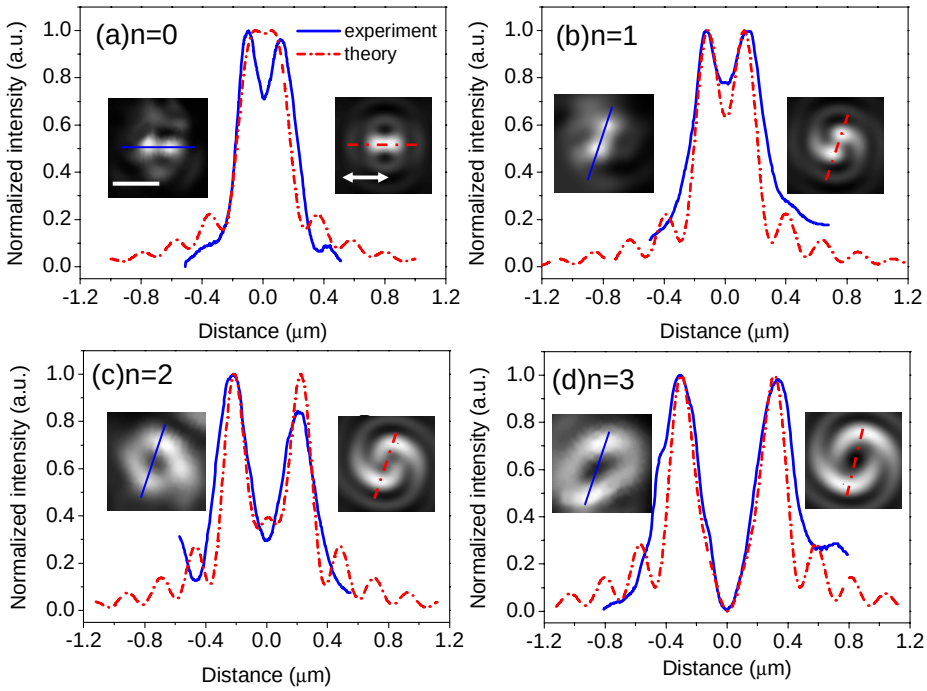

Fig. 4. Comparison between the experimental cross-sections of the normalized intensity distributions in the focal region of an objective with NA=1.65 at the coverglass (n_1=1.78) and air (n_2=1) interface for LG beams with n=0-3 with the theoretical calculations (a) along the incident polarization direction, (b-d) across the two peak intensity points. The insets on the left side of each Fig. show the measured focal intensity distributions, On the right side the theoretical simulations are presented. The arrow indicates the incident polarization direction. Scale bar: 500 nm.

#8834 - $15.00 USD Received 20 September 2005; revised 4 December 2005; accepted 5 December 2005
(C) 2005 OSA

4. Conclusion

In conclusion, a new phenomenon showing a focal spot rotation which occurs under the tight focus of an LG beam by a high NA TIR objective has been theoretically investigated using the vectorial Debye theory and experimentally mapped using a SNOM probe. The experimental measurements agree well with the theoretical predications. It has been proved that such a field distribution is directly resulted from the mixed effect of the helical phase of an LG beam and the phase shift induced by the total internal reflection when the beam passes the interface. Similar to the helical-conical beams [25], the asymmetric property of a focused LG beam may possess orbital angular momentum and facilitate a new mechanism for rotating micro-sized objects in near-field optical trapping.

Acknowledgments

The authors thank the Australian Research Council for its support.

#8834 - $15.00 USD Received 20 September 2005; revised 4 December 2005; accepted 5 December 2005
(C) 2005 OSA